Analysis and experimental concepts of the vibrating wire alignment technique

WANG Xiao-Long(王小龙)[1,2] DONG Lan(董岚)[1,2] WU Lei(吴蕾)[3,4] LI Chun-Hua(李春华)[3]

[1] China Spallation Neutron Source (CSNS), Institute of High Energy Physics (IHEP), Chinese Academy of Sciences (CAS), Dongguan 523803, China
[2] Dongguan Institute of Neutron Science (DINS), Dongguan 523808, China
[3] Institute of High Energy Physics, Chinese Academy of Sciences, Beijing 100049, China
[4] University of Chinese Academy of Sciences, Beijing 100049, China

Abstract: The vibrating wire alignment technique is a method which, by measuring the spatial distribution of a magnetic field, can achieve very high alignment accuracy. The vibrating wire alignment technique can be applied to fiducializing magnets and the alignment of accelerator straight section components, and it is a necessary supplement to conventional alignment methods. This article gives a systematic summary of the vibrating wire alignment technique, including vibrating wire model analysis, system frequency calculation, wire sag calculation, and the relation between wire amplitude and magnetic induction intensity. On the basis of this analysis, this article outlines two existing alignment methods, one based on magnetic field measurement and the other on amplitude and phase measurements. Finally, some basic experimental issues are discussed.

Key words: vibrating wire, alignment, magnetic field measurement, accelerator, magnet

PACS: 29.20.db, 06.60.Sx, 46.80.+j **DOI:** 10.1088/1674-1137/38/11/117010

1 Introduction

The vibrating wire alignment technique was first put forward by Alexander Temnykh of Cornell University. Inspired by the 'pulsed-wire' method [1], he suggested using vibrating wire for accelerator magnet alignment [2]. Compared with the pulsed-wire method, vibrating wire can substantially shorten the wire required for field measurements, which makes it possible to apply vibrating wire to the alignment of long straight section components in an accelerator. Compared with pulsed-wire, another advantage of vibrating wire is that no pulse current needs to be generated to pass through the long wire, so it becomes more convenient to use.

To do the alignment, the vibrating wire alignment technique measures the spatial distribution of the magnetic field, rather than using the mechanical structure of the magnets, as done in the conventional alignment method. Because it measures the magnetic field to find the center and establish the relation between the center and the fiducials, the vibrating wire method can substantially decrease the introduction of errors and achieve very high accuracy. The Brookhaven National Laboratory (BNL) reports that the vibrating wire method can align 6m straight section components within 0.03 mm [3], which is impossible for the conventional alignment method. The vibrating wire method can be applied to fiducialize magnets, align several magnet centers in a line [4], and align magnets in a cryostat [5]. The vibrating wire method can achieve high accuracy in a relatively small range and, if combined with some conventional alignment methods, it can effectively improve alignment accuracy for the whole accelerator complex.

2 Vibrating wire model analysis

The vibrating wire system is shown in Fig. 1. A thin wire is passed through the center of the magnet, the ends of which are fixed to the motor-driven translation stages. The stages can move along the x and y directions. The tension of the wire is T, a current $I(t)$ is passed through the wire, and at the end of the wire two sensors are used to measure the wire movement in the x and y directions.

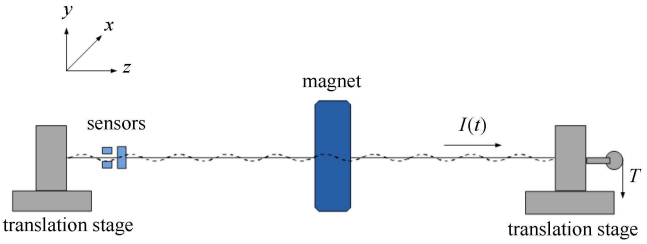

Fig. 1. Vibrating wire system.

Received 26 September 2013

This system can be seen as a typical forced string vibration model. The driving force is a Lorentz force generated by the current and magnetic field, and the frequency of the driving force is determined by the frequency of the current. It can be analyzed using standard forced string vibration methods [6].

As it carries alternating current, the wire in this model will be affected by stress, gravity, damping force and Lorentz force. We first analyze its movement in the y direction. For each point in the wire, its y coordinate is a function of coordinate z and time t, written as $y(z,t)$. The analysis of stress on a section of wire of length dz is shown in Fig. 2.

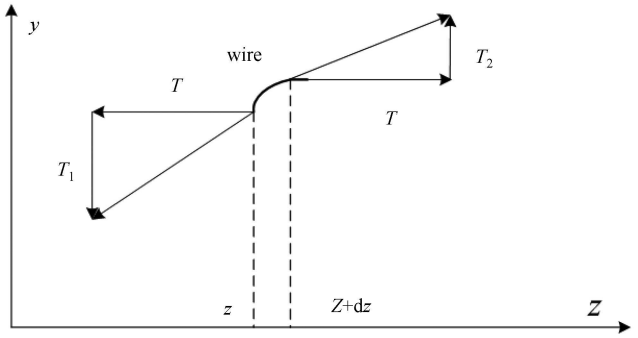

Fig. 2. Analysis of stress for a section of wire of length dz.

The dz segment will not move in the z direction, so the total force in the z direction is 0. In the y direction, on the left-hand side the force is $T_1=T\left(\frac{\partial y}{\partial z}\right)\Big|_z$, and on the right-hand side the force is $T_2=T\left(\frac{\partial y}{\partial z}\right)\Big|_{z+\mathrm{d}z}$. Then, the total force on dz is

$$T_2-T_1=T\left(\frac{\partial y}{\partial z}\right)\Big|_{z+\mathrm{d}z}-T\left(\frac{\partial y}{\partial z}\right)\Big|_z=T\int_z^{z+\mathrm{d}z}\frac{\partial^2 y}{\partial z^2}\mathrm{d}z.$$

When the length of dz is small enough, it can be written as $T_2-T_1=T\frac{\partial^2 y}{\partial z^2}\mathrm{d}z$. The gravity on d$z$ is $-\mu g\mathrm{d}z$, where μ is the density of the wire and g is the acceleration due to gravity. The damping force on the dz segment is $-\gamma\frac{\partial y}{\partial t}\mathrm{d}z$, where γ is the damping coefficient. The Lorentz force on the dz segment is $I(t)B_x(z)\mathrm{d}z$, where $I(t)$ is the driving current and $B_x(z)$ is the magnetic induction intensity in the x direction. So the differential equation of motion for segment dz is

$$\mu\mathrm{d}z\frac{\partial^2 y}{\partial t^2}=T\frac{\partial^2 y}{\partial z^2}\mathrm{d}z-\mu g\mathrm{d}z-\gamma\frac{\partial y}{\partial t}\mathrm{d}z+I(t)B_x(z)\mathrm{d}z.$$

Dividing through by dz and rearranging terms gives

$$\mu\frac{\partial^2 y}{\partial t^2}+\gamma\frac{\partial y}{\partial t}-T\frac{\partial^2 y}{\partial z^2}=-\mu g+I(t)B_x(z). \tag{1}$$

This is a nonhomogeneous second-order differential equation and will be discussed further below.

2.1 Natural frequency of the wire

When no forces act on the wire, from Eq. (1) we can get

$$\mu\frac{\partial^2 y}{\partial t^2}+\gamma\frac{\partial y}{\partial t}-T\frac{\partial^2 y}{\partial z^2}=0. \tag{2}$$

Because z and t are two independent variables, by separation of variables $y(z,t)=Y_z(z)Y_t(t)$, we then get

$$\frac{1}{TY_t}\left(\mu\frac{\mathrm{d}^2Y_t}{\mathrm{d}t^2}+\gamma\frac{\mathrm{d}Y_t}{\mathrm{d}t}\right)=\frac{1}{Y_z}\frac{\mathrm{d}^2Y_z}{\mathrm{d}z^2}. \tag{3}$$

Since both sides are functions of different variables, they must be constants. We set this constant equal to $-k^2$. From the right side of Eq. (3) we can get

$$\frac{\mathrm{d}^2Y_z}{\mathrm{d}z^2}+k^2Y_z=0. \tag{4}$$

Eq. (4) is a second-order homogeneous linear differential equation with constant coefficients, with a characteristic equation of $r^2+pr+q=0$, where $p=0$ and $q=k^2$. The solutions are $r=\pm\mathrm{i}k$. The solution of Eq. (4) is then $Y_z=C_1\sin kz+C_2\sin kz$. With the boundary conditions $Y_z(0)=Y_z(L)=0$, we can get $C_1=0$, $k=n\pi/L$. So, $Y_z(z)=C_2\sin\left(\frac{n\pi z}{L}\right)$, where $n=1, 2, 3\cdots$, and C_2 is an arbitrary constant. From the left side of Eq. (3) we can get

$$\frac{\mathrm{d}^2Y_t}{\mathrm{d}t^2}+\frac{\gamma}{\mu}\frac{\mathrm{d}Y_t}{\mathrm{d}t}+\frac{T}{\mu}\left(\frac{n\pi}{L}\right)^2Y_t=0. \tag{5}$$

By setting $\alpha=\frac{\gamma}{\mu}$, and $\omega_n^2=\frac{T}{\mu}\left(\frac{n\pi}{L}\right)^2$ we can get

$$\frac{\mathrm{d}^2Y_t}{\mathrm{d}t^2}+\alpha\frac{\mathrm{d}Y_t}{\mathrm{d}t}+\omega_n^2Y_t=0. \tag{6}$$

This is a second-order homogeneous linear differential equation with constant coefficients in $Y_t(t)$, which has a characteristic equation of $r^2+\alpha r+\omega_n^2=0$. The solutions are a pair of conjugate complex roots, $r=-\frac{\alpha}{2}\pm\mathrm{i}\sqrt{\omega_n^2-\left(\frac{\alpha}{2}\right)^2}$. So the solution of Y_t is

$$Y_t=\mathrm{e}^{-\frac{\alpha}{2}t}\left[c_1\cos\left(\sqrt{\omega_n^2-\left(\frac{\alpha}{2}\right)^2}t\right)+c_2\sin\left(\sqrt{\omega_n^2-\left(\frac{\alpha}{2}\right)^2}t\right)\right],$$

where c_1, c_2 are constants. The general solution of Eq. (2) is

$$\begin{aligned}y(z,t)&=Y_z(z)Y_t(t)\\&=\sum_{n=1}^{\infty}\mathrm{e}^{-\frac{\alpha}{2}t}\left[c_1\cos\left(\sqrt{\omega_n^2-\left(\frac{\alpha}{2}\right)^2}t\right)\right.\\&\quad\left.+c_2\sin\left(\sqrt{\omega_n^2-\left(\frac{\alpha}{2}\right)^2}t\right)\right]\sin\left(\frac{n\pi z}{L}\right).\end{aligned} \tag{7}$$

From Eq. (7) it can be found that, when no forces act on the wire and when damping is zero ($\gamma=0$), the natural frequency of the wire is ω_n. Because the damping is very small, the natural frequency of the wire can be assumed to be $\omega_n=2\pi\frac{n}{2L}\sqrt{\frac{T}{\mu}}$ and the basic natural frequency is $\omega_1=2\pi\frac{1}{2L}\sqrt{\frac{T}{\mu}}$.

2.2 The sag of wire due to gravity

When only gravity acts on the wire, from Eq. (1) we can get

$$\mu\frac{\partial^2 y}{\partial t^2}+\gamma\frac{\partial y}{\partial t}-T\frac{\partial^2 y}{\partial z^2}=-\mu g. \tag{8}$$

Since the force due to gravity does not vary over time, we can get $\frac{\partial^2 y}{\partial z^2}=\frac{\mu g}{T}$. After integrating twice, we get

$$y(z)=\frac{\mu g}{2T}z^2+c_1 z+c_2.$$

With the boundary conditions $y(0)=0$, $y(L)=0$, that is the case where the wire is level, we then get

$$y(z)=\frac{\mu g}{2T}z(z-L). \tag{9}$$

A more common condition is that the wire is tilted, as shown in Fig. 3.

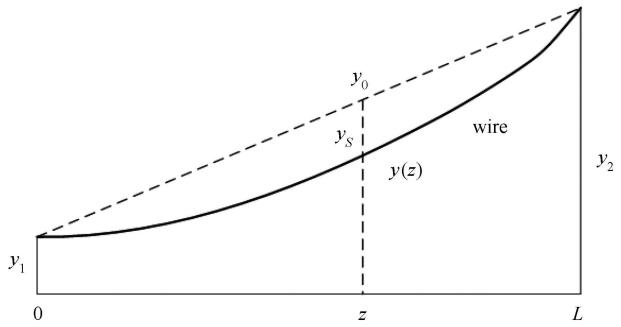

Fig. 3. Sag analysis of a tilted wire.

The boundary condition becomes $y(0)=y_1$, $y(L)=y_2$, so we get $y(z)=\frac{\mu g}{2T}z(z-L)+\frac{y_2-y_1}{L}z+y_1$. For $y_0(z)=\frac{y_2-y_1}{L}z+y_1$, the sag is then $y_S=y_0(z)-y(z)=-\frac{\mu g}{2T}z(z-L)$. This is as same as for the level wire. To calculate the maximum sag S, according to Eq. (9), setting $\frac{\mathrm{d}y}{\mathrm{d}z}=0$ gives $z=\frac{L}{2}$ $S=-\frac{\mu g L^2}{8T}$. For $\omega_1^2=\frac{\pi^2 T}{\mu L^2}$ we can then get $S=-\frac{g\pi^2}{8\omega_1^2}$. For $\omega_1=2\pi f_1$, where f_1 is the basic frequency, we can get $S=-\frac{g}{32f_1^2}$. By substituting into Eq. (9) we then get

$$y(z)=\frac{g}{8f_1^2L^2}z(z-L). \tag{10}$$

Eq. (10) is the sag equation. We can measure f_1 for the vibrating wire and then calculate the sag to do a sag correction.

2.3 The motion of wire driven by Lorentz force

When only the Lorentz force acts on the wire, from Eq. (1) we get

$$\mu\frac{\partial^2 y}{\partial t^2}+\gamma\frac{\partial y}{\partial t}-T\frac{\partial^2 y}{\partial z^2}=I(t)B_x(z). \tag{11}$$

According to the phasor representation method of electric circuit theory, the current can be written as $I(t)=I_0\mathrm{e}^{\mathrm{i}\omega t}$. When the vibration reaches a steady state, the vibration frequency will be the same as the driving force frequency [6], so we can set $y(z,t)=Y_\mathrm{B}(z)\mathrm{e}^{\mathrm{i}\omega t}$. Substituting into Eq. (11), we can get

$$-\omega^2\mu Y_\mathrm{B}\mathrm{e}^{\mathrm{i}\omega t}+\mathrm{i}\omega\gamma Y_\mathrm{B}\mathrm{e}^{\mathrm{i}\omega t}-T\frac{\mathrm{d}^2 Y_\mathrm{B}}{\mathrm{d}z^2}\mathrm{e}^{\mathrm{i}\omega t}=I_0\mathrm{e}^{\mathrm{i}\omega t}B_x(z).$$

By re-arranging this, we can get

$$-\omega^2\mu Y_\mathrm{B}+\mathrm{i}\omega\gamma Y_\mathrm{B}-T\frac{\mathrm{d}^2 Y_\mathrm{B}}{\mathrm{d}z^2}=I_0 B_x(z). \tag{12}$$

Eq. (12) is a very complicated differential equation, with $Y_\mathrm{B}(z)$ and $B_x(z)$ both being rather complicated functions of z. In order to easily solve Eq. (12), we can use the boundary conditions $Y_\mathrm{B}(0)=0$, $Y_\mathrm{B}(L)=0$, and expand $Y_\mathrm{B}(z)$ and $B_x(z)$ in a Fourier sine series:

$$Y_\mathrm{B}(z)=\sum_{n=1}^{\infty}Y_{\mathrm{B}n}\sin\Big(\frac{n\pi z}{L}\Big), \tag{13}$$

where $Y_{\mathrm{B}n}$ is a constant;

$$B_x(z)=\sum_{n=1}^{\infty}B_{xn}\sin\Big(\frac{n\pi z}{L}\Big), \tag{14}$$

where B_{xn} is a constant. Substituting these in Eq. (12) we can get

$$\begin{aligned}&-\omega^2\mu\left(\sum_{n=1}^{\infty}Y_{\mathrm{B}n}\sin\Big(\frac{n\pi z}{L}\Big)\right)\\&+\mathrm{i}\omega\gamma\left(\sum_{n=1}^{\infty}Y_{\mathrm{B}n}\sin\Big(\frac{n\pi z}{L}\Big)\right)\\&+T\left(\sum_{n=1}^{\infty}Y_{\mathrm{B}n}\sin\Big(\frac{n\pi z}{L}\Big)\Big(\frac{n\pi}{L}\Big)^2\right)\\&=I_0\left(\sum_{n=1}^{\infty}B_{xn}\sin\Big(\frac{n\pi z}{L}\Big)\right).\end{aligned}$$

For arbitrary n,

$$\left[-\omega^2+\mathrm{i}\omega\frac{\gamma}{\mu}+\frac{T}{\mu}\Big(\frac{n\pi}{L}\Big)^2\right]Y_{\mathrm{B}n}=\frac{1}{\mu}I_0 B_{xn}.$$

By setting $\alpha=\frac{\gamma}{\mu}$, $\omega_n^2=\frac{T}{\mu}\left(\frac{n\pi}{L}\right)^2$ we can get

$$Y_{\mathrm{B}n}=\frac{-I_0B_{xn}}{\mu(\omega^2-\omega_n^2-\mathrm{i}\omega\alpha)}.$$

Then

$$Y_{\mathrm{B}}(z)=\sum_{n=1}^{\infty}\frac{-I_0B_{xn}}{\mu(\omega^2-\omega_n^2-\mathrm{i}\omega\alpha)}\sin\left(\frac{n\pi z}{L}\right).$$

Using the complex solution method for vibration differential equations, $y(z,t)$ is equal to the real part of $Y_{\mathrm{B}}(z)\mathrm{e}^{\mathrm{i}\omega t}$:

$$\begin{aligned}y(z,t) &= \mathrm{Re}\sum_{n=1}^{\infty}\frac{-I_0B_{xn}}{\mu(\omega^2-\omega_n^2-\mathrm{i}\omega\alpha)}\sin\left(\frac{n\pi z}{L}\right)\mathrm{e}^{\mathrm{i}\omega t}\\ &=\sum_{n=1}^{\infty}\frac{-I_0B_{xn}\sin\left(\frac{n\pi z}{L}\right)}{\mu\left[(\omega^2-\omega_n^2)^2+(\omega\alpha)^2\right]}[(\omega^2-\omega_n^2)\cos(\omega t)\\ &\quad -\omega\alpha\sin(\omega t)].\end{aligned}\tag{15}$$

The motion of the wire in the x direction is similar to that in the y direction, but in the x direction gravity does not act on the wire and the Lorentz force is generated by $B_y(z)$. It can thus be seen that the natural frequency in the x direction is the same as that in the y direction and gravity does not need to be considered. The equation for the Lorentz force in the x direction can be obtained by substituting B_{xn} for B_{yn} in Eq. (15). This completes the analysis of the vibrating wire model.

3 Magnet alignment

Eq. (15) describes the relationship between the motion of point z in the y direction and the magnetic induction intensity B_{xn}, but Eq. (15) is still too complex and difficult to be applied in actual measurements. It needs to be further simplified for practical application.

3.1 Magnet alignment based on the distribution of magnetic field measurement

Alexander Temnykh provided a method for magnet alignment by measuring the distribution of the magnetic induction intensity in the x-y cross section [2, 7]. Taking the y direction as an example, we can construct a function

$$\mathcal{F}(\omega)=\frac{1}{T}\int_0^T y(z,t)\mathrm{Re}\left(I_0\mathrm{e}^{\mathrm{i}\omega t}\right)\mathrm{d}t,\tag{16}$$

where T is the sampling time, which should be integral multiple of the current cycle; $y(z,t)$ is the amplitude of point z on the wire in the y direction; and, $I_0\mathrm{e}^{\mathrm{i}\omega t}$ is the current. $\mathcal{F}(\omega)$ can be found by measurement. By setting the position of the sensor as z, the sensor samples the motion of the wire in the y direction during period T, simultaneously sampling the current. These data are then used to integrate Eq. (16) numerically. The sampling rate can be selected according to the fastest sampling rate of the instrument.

In order to measure the distribution of the magnetic induction intensity in the x-y cross section, the wire should be used to do scan measurements in both the x and y directions. Taking the y direction as an example, we should firstly use a conventional alignment method to align the wire to the center of the magnet with an accuracy of 0.1 mm, we can be sure that the center of magnet must be within 1 mm of the wire. Secondly, by taking the wire's current position as the center and selecting a series of points in a 2 mm wide range in the y direction, a frequency scan measurement is done at each point. When doing the frequency scan measurement, we should set one natural frequency as the center and use a series of currents with frequencies close to that central frequency to measure $\mathcal{F}(\omega)$. We can then get a graph of $\mathcal{F}(\omega)$-ω. Fig. 4 shows the scan result for one of these points.

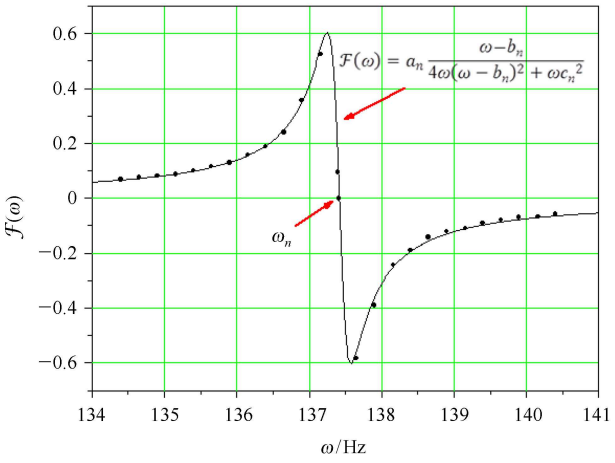

Fig. 4. Frequency scan.

Through the frequency scan we can get the magnetic induction intensity at this point. By substituting the $y(z,t)$ in Eq. (16) with Eq. (15), we get

$$\begin{aligned}\mathcal{F}(\omega) &= \sum_{n=1}^{\infty}\frac{-I_0^2B_{xn}\sin\left(\frac{n\pi z}{L}\right)(\omega^2-\omega_n^2)}{2\mu\left[(\omega^2-\omega_n^2)^2+(\omega\alpha)^2\right]}\\ &=\sum_{n=1}^{\infty}\frac{-I_0^2B_{xn}\sin\left(\frac{n\pi z}{L}\right)(\omega+\omega_n)(\omega-\omega_n)}{2\mu\left[(\omega+\omega_n)^2(\omega-\omega_n)^2+(\omega\alpha)^2\right]}.\end{aligned}$$

When ω is close to ω_n, this can be simplified to

$$\mathcal{F}(\omega) = \sum_{n=1}^{\infty}\frac{-I_0^2B_{xn}\sin\left(\frac{n\pi z}{L}\right)2\omega(\omega-\omega_n)}{2\mu\left[4\omega^2(\omega-\omega_n)^2+(\omega\alpha)^2\right]}$$

$$= \sum_{n=1}^{\infty} \frac{-I_0^2 B_{xn} \sin\left(\frac{n\pi z}{L}\right)(\omega-\omega_n)}{\mu\left[4\omega(\omega-\omega_n)^2+\omega\alpha^2\right]}. \quad (17)$$

We can set $\mathcal{F}(\omega)=\sum_{n=1}^{\infty}\mathcal{F}_n(\omega)$, where

$$\mathcal{F}_n(\omega)=\frac{-I_0^2 B_{xn}}{\mu}\sin\left(\frac{n\pi z}{L}\right)\frac{\omega-\omega_n}{4\omega(\omega-\omega_n)^2+\omega\alpha^2}. \quad (18)$$

Since a vibrating wire system is a weakly damped system, $\frac{\omega\alpha^2}{\omega-\omega_n}$ will become very small in a certain range. In Eq. (18), when $\omega\approx\omega_n$, $\mathcal{F}_n(\omega)$ will become very big, but when $\omega=\omega_n$, $\mathcal{F}_n(\omega)=0$. This can be seen in Fig. 4: when ω is close to ω_n, $\mathcal{F}(\omega)$ becomes very big, due to $\mathcal{F}_n(\omega)$ being much bigger than other terms, so when $\omega\approx\omega_n$, $\mathcal{F}(\omega)\approx\mathcal{F}_n(\omega)$.

We can simplify Eq. (18) as follows:

$$\mathcal{F}(\omega)=a_n\frac{\omega-b_n}{4\omega(\omega-b_n)^2+\omega c_n^2}, \quad (19)$$

where a_n, b_n, c_n are coefficients to be solved for. Comparing with (18), we can get $a_n=\frac{-I_0^2 B_{xn}}{\mu}\sin\left(\frac{n\pi z}{L}\right)$, $b_n=\omega_n$, $c_n=\alpha$. Solving for a_n can, therefore, allow us to calculate B_{xn}. By using (19) as the model equation and using the measured data to do nonlinear fitting we can get a_n. Before doing the fit we need to set the initial values for a_n, b_n, c_n. The initial value of b_n can be calculated from the equation $\omega_n=2\pi\frac{n}{2L}\sqrt{\frac{T}{\mu}}$, but a_n and c_n do not have such equations. We can calculate the initial values of a_n and c_n by rearranging Eq. (19) to give

$$\frac{1}{\mathcal{F}(\omega)}=x_1\times 4\omega^2-x_2\times 4\omega+x_3\times\frac{\omega}{\omega-b_n}, \quad (20)$$

where $x_1=\frac{1}{a_n}$ $x_2=\frac{b_n}{a_n}$ $x_3=\frac{c_n^2}{a_n}$. By substituting b_n in (20) with its initial value, through linear fitting we can solve for x_1, x_2, and x_3 and then calculate the initial values of a_n and c_n. The result of nonlinear fitting is shown in Fig. 4. According to (14), if we measure many orders of B_n, we can approximately calculate B_x at the wire location.

After doing the frequency scan at every point we will get the distribution of magnetic induction intensity in the y direction, as shown in Fig. 5. From Fig. 5 it can be found that the magnetic center is at 0.1 mm. The measurement of magnetic induction intensity in the x direction is done in the same way as for the y direction but instead using the sensor measure $x(z,t)$ and the magnetic induction intensity $B_y(z)$.

For magnet alignment, one needs not only to align the magnetic center but also to align the roll, pitch, and yaw. The vibrating wire method cannot measure roll, so we should use the conventional method for roll alignment, but a vibrating wire can be used to measure pitch and yaw. According to (14), through measuring many orders of B_n, we can approximately calculate $B(z)$. The relationship between $B(z)$ and quadrupole position is shown in Fig. 6.

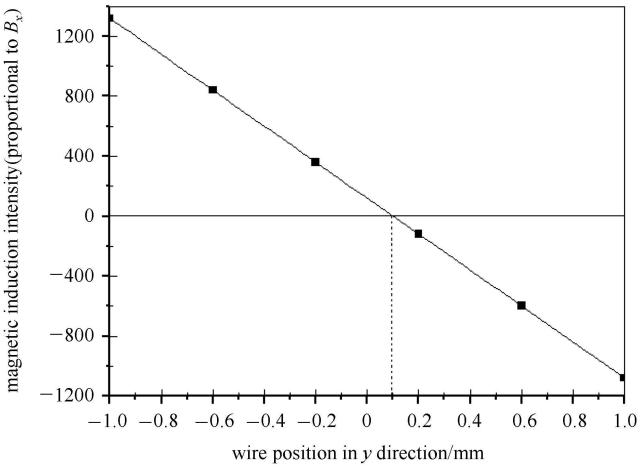

Fig. 5. Distribution of magnetic induction intensity.

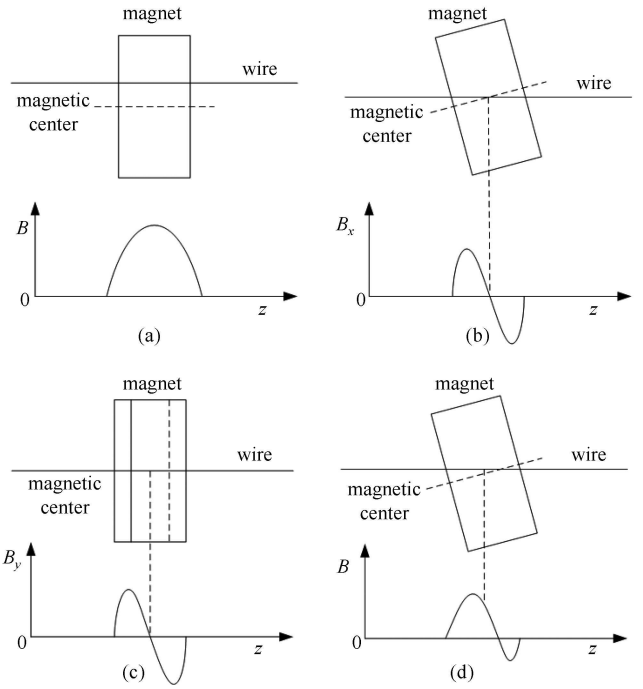

Fig. 6. Relationship between $B(z)$ and magnet position: (a) shift measurement; (b) pitch measurement; (c) yaw measurement; and, (d) shift and tilt measurement.

When pitch and yaw are zero and the magnetic center is on the wire, $B(z)$ should also be zero. When pitch and yaw are zero and the magnetic center is not on the wire, $B(z)$ should be as shown in Fig. 6(a), with a peak at

the magnet center location. When only the pitch is non-zero, $B_x(z)$ should be as shown in Fig. 6(b), with two symmetrical peaks of different polarities at the magnet location. When only the yaw is non-zero, $B_y(z)$ should be as shown in Fig. 6(c), with two symmetrical peaks of different polarities at the magnet location. When tilt and shift are both non-zero, $B(z)$ should be as shown in Fig. 6(d), with two asymmetrical peaks of different polarities at the magnet location. One thing to be noticed is that the accuracy of $B(z)$ is determined by the highest order of B_n measured because the higher the order the shorter the wavelength and, hence, the more accurate the description of $B(z)$. If the wavelength of the highest order B_n is longer than the magnet, then the result in Fig. 6 will not be obtained.

3.2 Magnet alignment based on amplitude and phase measurement

Zachary Wolf provided a method of quadrupole alignment by measuring wire amplitude and phase [8]. According to the theory of forced vibrations, for a weakly damped system, when the drive force frequency ω is the same as one of the system natural frequencies ω_k the system will generate resonance [6]. When there is resonance, the $n=k$ term in Eq. (15) will be much bigger than the other terms and for any point of the wire its motion phase will lag the drive force by $\frac{\pi}{2}$, so (15) can be simplified as

$$y(z,t)\approx\frac{I_0 B_{xn}}{\mu\omega_n\alpha}\sin\left(\frac{n\pi z}{L}\right)\cos\left(\omega_n t-\frac{\pi}{2}\right). \tag{21}$$

Taking the y direction as an example, to find the magnetic center of the magnet, we first use conventional alignment methods to align the wire to the center of the magnet and then select a natural frequency ω_n as the driving current frequency. In order to get the actual resonance frequency, we need to monitor the wire motion phase and the driving current phase, adjust the current frequency until the wire phase lags the current phase by $\frac{\pi}{2}$, and then use a lock-in amplifier to get the resonance frequency. For a quadrupole magnet, $B_x=Gy_{\rm d}$, where G is the magnetic field gradient, $y_{\rm d}$ is the distance between the wire and the magnetic center in the y direction. To get the value of $y_{\rm d}$, we need to deduce the relationship between $y_{\rm d}$ and B_{xn} and substitute it into (22) to solve.

Using a Fourier transformation,

$$B_{xn}=\frac{2}{L}\int B_x(z)\sin\left(\frac{n\pi z}{L}\right)\mathrm{d}z.$$

Setting the effective length of magnetic field as $L_{\rm m}$, the magnetic center location in the z direction is $z_{\rm m}=\frac{L}{j}$. When the tilt of the magnet relative to the wire is very small, $B_x(z)$ can be seen as a constant B_x, so

$$\begin{aligned}B_{xn} &= \frac{2}{L}\int_{\frac{L}{j}-\frac{L_{\rm m}}{2}}^{\frac{L}{j}+\frac{L_{\rm m}}{2}} B_x\sin\left(\frac{n\pi z}{L}\right)\mathrm{d}z\\ &= -\frac{2}{L}B_x\frac{L}{n\pi}\cos\left(\frac{n\pi z}{L}\right)\Bigg|_{\frac{L}{j}-\frac{L_{\rm m}}{2}}^{\frac{L}{j}+\frac{L_{\rm m}}{2}}\\ &= \frac{4B_x}{n\pi}\sin\left(\frac{n\pi}{j}\right)\sin\left(\frac{n\pi}{2}\frac{L_{\rm m}}{L}\right)\\ &= \frac{4Gy_{\rm d}}{n\pi}\sin\left(\frac{n\pi}{j}\right)\sin\left(\frac{n\pi}{2}\frac{L_{\rm m}}{L}\right).\end{aligned} \tag{22}$$

Substituting into (21).

$$\begin{aligned}y(z,t) \approx \frac{I_0 4Gy_{\rm d}}{\mu\omega_n\alpha n\pi}&\sin\left(\frac{n\pi}{j}\right)\sin\left(\frac{n\pi}{2}\frac{L_{\rm m}}{L}\right)\sin\left(\frac{n\pi z}{L}\right)\\ &\times\cos\left(\omega_n t-\frac{\pi}{2}\right).\end{aligned}$$

The relation between the maximum amplitude $y_{\max}(z)$ and $y_{\rm d}$ is therefore

$$\begin{aligned}y_{\max}(z) = \Bigg[\frac{I_0 4G}{\mu\omega_n\alpha n\pi}&\sin\left(\frac{n\pi}{j}\right)\sin\left(\frac{n\pi}{2}\frac{L_{\rm m}}{L}\right)\\ &\times\sin\left(\frac{n\pi z}{L}\right)\Bigg]|y_{\rm d}|.\end{aligned} \tag{23}$$

Using (23) the magnetic center in the y direction can be calculated by measuring $y_{\max}(z)$.

The measurement of the magnetic center in the x direction is the same as the y direction, but with $x(z,t)$ used as the sensor measurement and $B_y(z)$ as the magnetic induction intensity.

For quadrupoles, the directions of magnetic induction intensity on both sides of the magnet center are opposite as shown in Fig. 7.

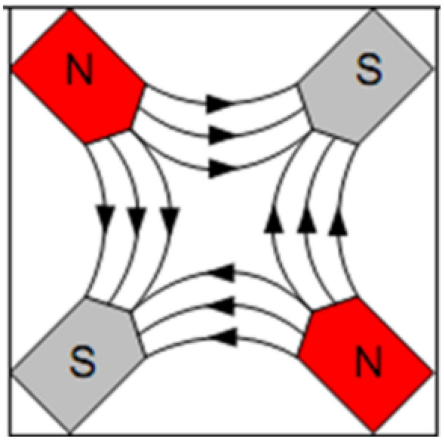

Fig. 7. Quadrupole magnetic field.

Correspondingly, the phase of the wire relative to the driving current will also change, from $-\frac{\pi}{2}$ to $\frac{\pi}{2}$ or from

$\frac{\pi}{2}$ to $-\frac{\pi}{2}$. By monitoring the wire phase change, we can judge which side the wire is on. Taking the y direction as an example, the relationship of the wire motion phase ϕ and $y_{\rm d}$ is ϕ=$-$sign$(y_{\rm d})\left(\frac{\pi}{2}\right)$.

When the tilt of the magnet relative to the wire is not small and tilt alignment is needed, $B(z)$ at the wire location will not be seen as a constant; it should be expressed as a function of the tilt θ Taking quadrupole pitch as an example, after finishing the alignment in the x and y directions, the pitch alignment should be done as shown in Fig. 8.

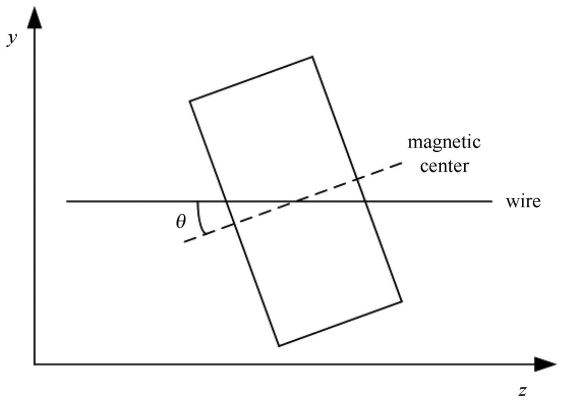

Fig. 8. Quadrupole pitch alignment.

$$B_x(z)=-G\left(z-\frac{L}{j}\right)\tan\theta\approx-G\left(z-\frac{L}{j}\right)\theta,$$

$$\begin{aligned}B_{xn} &= \frac{2}{L}\int_{\frac{L}{j}-\frac{L_{\rm m}}{2}}^{\frac{L}{j}+\frac{L_{\rm m}}{2}} B_x(z)\sin\left(\frac{n\pi z}{L}\right)\mathrm{d}z\\ &= \frac{2}{L}\int_{\frac{L}{j}-\frac{L_{\rm m}}{2}}^{\frac{L}{j}+\frac{L_{\rm m}}{2}} -G\left(z-\frac{L}{j}\right)\theta\sin\left(\frac{n\pi z}{L}\right)\mathrm{d}z\\ &= \frac{2G}{L}\left[\frac{L_{\rm m}L}{n\pi}\cos\frac{n\pi}{j}\cos\frac{n\pi L_{\rm m}}{2L}\right.\\ &\quad\left.-2\left(\frac{L}{n\pi}\right)^2\cos\frac{n\pi}{j}\sin\frac{n\pi L_{\rm m}}{2L}\right]\theta.\end{aligned}$$

Substituting into (21).

$$\begin{aligned}y(z,t) \approx\ & \frac{I_0 2G}{\mu\omega_n\alpha L}\left[\frac{L_{\rm m}L}{n\pi}\cos\frac{n\pi}{j}\cos\frac{n\pi L_{\rm m}}{2L}\right.\\ &\left.-2\left(\frac{L}{n\pi}\right)^2\cos\frac{n\pi}{j}\sin\frac{n\pi L_{\rm m}}{2L}\right]\\ &\times\theta\sin\left(\frac{n\pi z}{L}\right)\cos\left(\omega_n t-\frac{\pi}{2}\right).\end{aligned}$$

So the relation of $y_{\max}(z)$ and θ is

$$\begin{aligned}y_{\max}(z) =\ & \frac{I_0 2G}{\mu\omega_n\alpha L}\left[\frac{L_{\rm m}L}{n\pi}\cos\frac{n\pi}{j}\cos\frac{n\pi L_{\rm m}}{2L}\right.\\ &\left.-2\left(\frac{L}{n\pi}\right)^2\cos\frac{n\pi}{j}\sin\frac{n\pi L_{\rm m}}{2L}\right]\sin\left(\frac{n\pi z}{L}\right)|\theta|.\end{aligned} \tag{24}$$

The relation between the wire motion phase relative to the driving current ϕ and θ is ϕ=sign$(\theta)\left(\frac{\pi}{2}\right)$. For θ>0, $\phi=\frac{\pi}{2}$ and for θ<0, $\phi=-\frac{\pi}{2}$. The yaw measurement method is the same as for pitch, but with the sensor measuring $x(z,t)$ and the magnetic induction intensity being $B_y(z)$.

4 Some basic experimental techniques

4.1 Sensor

The sensor used in the vibrating wire method is a kind of optical chopper, as shown in Fig. 9.

Its output characteristic is shown in Fig. 10.

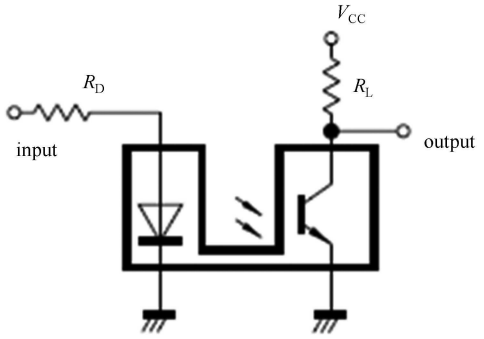

Fig. 9. Optical chopper.

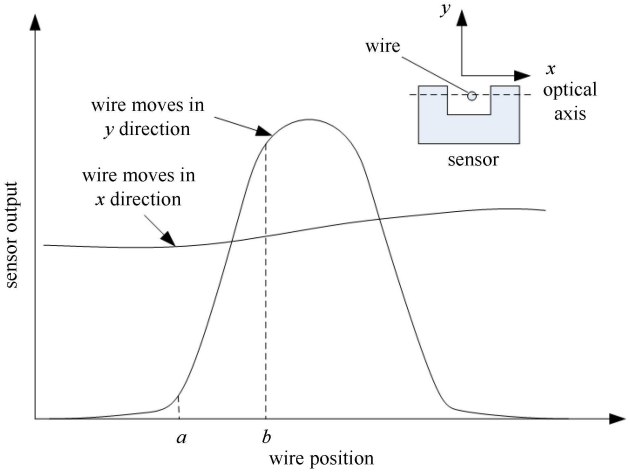

Fig. 10. Sensor output characteristic.

When the wire moves between a and b, its output and motion have a linear relation. We should, therefore, control the amplitude of the wire at the sensor position in order to make it smaller than the distance between a and b. The sensor output is sensitive to the direction of wire movement, so we need to use two sensors to monitor the wire motion in x and y, respectively.

4.2 Wire

The wire used in the vibrating wire system must be non-magnetic. We chose Cu-2% Be wire. The diameter of the wire should be about 0.1 mm. If it is too thick it will increase the damping, while if it is too thin it will decrease its tensile strength.

4.3 Driving current frequency

From Section 3.1, by measuring the magnetic induction intensity components we can calculate the magnetic induction intensity, but we do not need to measure many components, just some of the most representative. From Eq. (14) it can be seen when $n=\dfrac{(1+2k)L}{2z_{\rm m}}$ (k=0, 1, 2, $\cdots$, $z_{\rm m}$ is the magnet z coordinate), the nth order component is the biggest one at the magnet location, so we can use this to choose the driving current frequency.

According to Eq. (22), when $z_{\rm m}=\dfrac{(1+2k)L}{2n}$ (k =0, 1, 2, $\cdots$, $z_{\rm m}$ is magnet z coordinate) B_{xn} reaches its biggest value. From Eq. (21) the wire's biggest amplitude $y_{\max}(z)$ is proportional to B_{xn}, so using the location of the magnet to choose the driving current frequency can improve the measurement accuracy. In conclusion, we should make sure that the magnet is located at the peak of the wire nth order vibrating mode.

4.4 Sag correction

The nominal reference shape for a vibrating wire is the straight line between the ends of the wire, but in reality the wire follows a catenary curve because of gravity. We therefore need to correct for the sag. According to Eq. (10), by measuring the basic frequency we can calculate for the sag at the magnet center and then, after subtracting the sag value from the magnetic center value in the y direction, we can get the distance between the magnetic center and the nominal reference line.

4.5 Background field elimination

The vibrating wire alignment technique is based on magnetic field measurements, but in actual measurement the magnetic fields acting on the wire come not only from the magnet under measurement but also from other magnets nearby, as well as the earth's magnetic field. In order to eliminate these magnetic fields we can first use the vibrating wire to do a scan measurement within the measurement range when the magnets are switched off. We can thus get the background field distribution. Through best-fit procedures we can get the magnetic induction intensity distribution curves in the x and y directions relative to the wire position. Then, with the magnet switched on, the scan measurement is repeated and best-fit procedures are performed to get the distribution curves with the magnet powered on. Subtracting the power-off curve from the power-on curve then gives the magnetic field with the background fields eliminated.

5 Conclusions

The vibrating wire alignment technique is a kind of high accuracy alignment technique that can be applied to fiducializing components or the alignment of straight section components, which is a necessary supplement to the conventional alignment method. In this article we analyzed the vibrating wire mode in detail, deduced the resonance frequency equation, sag equation and wire amplitude and magnetic induction intensity relation equations. We then presented two kinds of alignment method, and finally discussed some basic experimental techniques.

References

1 Fortgang C M. Pulsed Taut-Wire Alignment of Multiple Permanent Magnet Quadrupoles. LINAC Conf., Albuquerque NM, September 1990
2 Temnykh Alexander. Nuclear Instrument and Methods in Physics Research A, 1997, **399**: 185–194
3 Jain Animesh. Results from Vibrating Wire R&D for Alignment of Multipoles in NSLS-Ⅱ. 16th International Magnetic Measurement Workshop. 2009
4 Jain A, Anerella M, Ganetis G et al. Vibrating Wire R&D for Alignment of Multipole Magnets in NSLS-Ⅱ. The 10th International Workshop on Accelerator Alignment. 2008
5 Temnykh Alexander. The Use of Vibrating Wire Technique for Precise Positioning of CESR Phase Ⅲ Super-Conducting Quadrupoles at Room Temperature. Proceeding of the 2001 Particle Accelerator Conference. Chicago, 2001. 3469–3471
6 Kittel C, Knight W D, Ruderman M A et al. Berkeley Physics Course. Beijing: Science Press, 1979
7 Temnykh Alexander. The Magnetic Center Finding Using Vibrating Wire Technique. 11th International Magnetic Measurement Workshop. 1999
8 Wolf Zachary. A Vibrating Wire System for Quadrupole Fiducialization, SLAC-TN-10-087. 2010